

SLIDING-MODE OBSERVER FOR SENSORLESS CONTROL OF PERMANENT MAGNET SYNCHRONOUS MOTOR DRIVES

Gheorghe Daniel ANDREESCU

University "Politehnica" of Timisoara, Department of Automation and Industrial Informatics

Blvd. Vasile Parvan 2, 300223 Timisoara, Romania, E-mail: dandre@aut.utt.ro

Abstract: *The paper develops a robust sliding-mode based observer to estimate the speed and position in sensorless control of permanent magnet synchronous motor (PMSM) drives using only two phase-current sensors and one dc-link voltage sensor. The nonlinear observer structure contains two main parts. 1) A sliding-mode disturbance observer estimates the electromotive force vector as equivalent control using the PMSM electromagnetic model in stator reference and a speed-adaptive low-pass filter. 2) A phase-locked loop state-observer extracts the speed and position from the equivalent control using a variable-structure PI state-observer. A sensorless PMSM drive with current vector control using this observer is investigated by extensive digital simulation and by experimental tests. The results prove good dynamic performances in medium speed range from zero to rated transient torque, and robustness to real parameter variations.*

Keywords: *sliding mode, state observers, adaptive filters, phase-locked loop, permanent magnet motors, motor control.*

1. INTRODUCTION

Permanent magnet synchronous motor (PMSM) drives have been widely used as servo drives for their high performances: high torque density, high efficiency and small size.

The control of PMSMs with sinusoidal flux distribution requires the rotor position to synchronize the stator currents with the rotor position, and the mechanical speed for the speed control. Encoders or resolvers have been used for sensing these variables. However, these transducers are expensive and mechanically unreliable. Therefore, the position and speed

sensorless control using only terminal current and voltage sensors have been desired.

There are several estimation methods for sensorless control of PMSM drives [1-3]:

- 1) Full-order observer, reduced-order observers, extended Luenberger observers,
- 2) Hypothetical position approach,
- 3) Extended Kalman filters,
- 4) MRAS flux observers,
- 5) Flux observers with equivalent integrators,
- 6) Sliding mode based observers,
- 7) Signal injection methods.

The main difficulty is the observer sensitivity to parameter errors and disturbances, especially at low speed and in reverse speed at zero crossing.

PMSM has a nonlinear MIMO model, speed dependent, with time-varying parameters. Moreover, the motor voltage-source inverter (VSI) presents an inherent nature of variable structure system (VSS). Sliding mode based observers (SMO) are well matched to these kind of systems giving robustness against bounded disturbances, system parameter uncertainties and unmodeled dynamics [4-8]. The SMO realizes sliding modes only inside the observer but the estimated variables are filtered to attenuate the chattering. Unfortunately, there are phase-delays speed depending that affects the system stability and the position estimation.

This paper develops a robust state observer based on: 1) sliding-mode disturbance observer with adaptive filter for equivalence control - to estimate the electromotive force, combined with 2) a phase-locked loop technique - to estimate the speed and position in PMSM sensorless control. Extensive digital simulation results and also experimental tests are presented.

2. SLIDING-MODE DISTURBANCE OBSERVER

The observer structure depends on the controlled system model. Let be consider a class of MIMO systems with uncertain parameters and disturbance described by the state model [6]:

$$\begin{bmatrix} \dot{\mathbf{x}}_1 \\ \dot{\mathbf{x}}_2 \end{bmatrix} = \begin{bmatrix} \mathbf{A}_{11} & \mathbf{A}_{12} \\ \mathbf{A}_{21} + \Delta\mathbf{A}_{21} & \mathbf{A}_{22} + \Delta\mathbf{A}_{22} \end{bmatrix} \begin{bmatrix} \mathbf{x}_1 \\ \mathbf{x}_2 \end{bmatrix} + \begin{bmatrix} 0 \\ \mathbf{B}_2 + \Delta\mathbf{B}_2 \end{bmatrix} \mathbf{u} + \begin{bmatrix} 0 \\ \mathbf{f}(\mathbf{z}) \end{bmatrix}, \quad \begin{bmatrix} \mathbf{x}_1 \\ \mathbf{x}_2 \end{bmatrix}_{t=0} = \begin{bmatrix} \mathbf{x}_{10} \\ \mathbf{x}_{20} \end{bmatrix}, \quad (1)$$

where: $\mathbf{x}_1 \in \mathbf{R}^{n-m}$, $\mathbf{x}_2 \in \mathbf{R}^m$ – state vectors, $\mathbf{u} \in \mathbf{R}^m$ – input vector, \mathbf{A} , \mathbf{B} – nominal system matrices, $\Delta\mathbf{A}$, $\Delta\mathbf{B}$ – uncertain parameter matrices, $\mathbf{f}(\mathbf{z})$ – time variant function of unknown but bounded disturbance \mathbf{z} . The dynamic model component \mathbf{x}_1 (1st line) does not have direct input. The main goal is to estimate the disturbance \mathbf{z} .

A solution is a sliding mode based observer (SMO) [4] with discontinuous correction $\mathbf{v} \in \mathbf{R}^m$

$$\dot{\hat{\mathbf{x}}}_2 = \mathbf{A}_{21o}\mathbf{x}_1 + \mathbf{A}_{22o}\hat{\mathbf{x}}_2 + \mathbf{B}_{2o}(\mathbf{u} + \mathbf{v}), \quad \hat{\mathbf{x}}_2(0) = \hat{\mathbf{x}}_2(0). \quad (2)$$

The subscript "o" suggests SMO estimated matrices. The correction \mathbf{v} compensates unknown disturbances by a robust sliding-mode action. A simple discontinuous time switching function as relay (3) is chosen for \mathbf{v} that leads

the system (2) to a sliding-mode evolution [4], [9] in the state space on the switching surface $\boldsymbol{\sigma}$.

$$\mathbf{v} = U_0 \text{sign}(\boldsymbol{\sigma}), \quad U_0 > 0. \quad (3)$$

$$\boldsymbol{\sigma} = \mathbf{e} = \mathbf{x}_2 - \hat{\mathbf{x}}_2 = \mathbf{0}. \quad (4)$$

$\boldsymbol{\sigma}$ is naturally selected to be (4) because the asymptotic stability of the observer (2) means $\hat{\mathbf{x}}_2 \rightarrow \mathbf{x}_2$ as soon as possible in dynamic regime; this is one of the state observer goals.

The sliding mode occurs in the switching surface vicinity if the condition for existence and reachability of the sliding mode (5) is fulfilled [4], resulting also the constraint for U_0 .

$$\boldsymbol{\sigma} \dot{\boldsymbol{\sigma}} < \mathbf{0}. \quad (5)$$

In the ideal tuned case (6) the state-error dynamic equation (7) results from (1) and (2).

$$\mathbf{A}_{21o} = \mathbf{A}_{21}, \quad \mathbf{A}_{22o} = \mathbf{A}_{22}, \quad \mathbf{B}_{2o} = \mathbf{B}_2. \quad (6)$$

$$\dot{\mathbf{e}} = \mathbf{A}_{22}\mathbf{e} + \Delta\mathbf{A}_{21}\mathbf{x}_1 + \Delta\mathbf{A}_{22}\mathbf{x}_2 + \Delta\mathbf{B}_2\mathbf{u} + \mathbf{f}(\mathbf{z}) - \mathbf{B}_2\mathbf{v} \quad (7)$$

The equivalent control \mathbf{v}_{eq} (8) estimates the equivalent-disturbance [4], [9] obtained in ideal sliding mode as $\mathbf{v}_{\text{eq}} = \mathbf{v}$, with $\mathbf{e} = \mathbf{0}$ and $\dot{\mathbf{e}} = \mathbf{0}$.

$$\mathbf{B}_2\mathbf{v}_{\text{eq}} = \Delta\mathbf{A}_{21}\mathbf{x}_1 + \Delta\mathbf{A}_{22}\mathbf{x}_2 + \Delta\mathbf{B}_2\mathbf{u} + \mathbf{f}(\mathbf{z}). \quad (8)$$

Because the dynamic system component \mathbf{x}_1 from (1) is without direct input, and \mathbf{A}_{11} is negative definite, then in (8) the term $\Delta\mathbf{A}_{21}\mathbf{x}_1$ could be missed and also in SMO (2) [6].

The physical meaning regarding the equivalent control \mathbf{v}_{eq} is one of the keys in this approach: \mathbf{v}_{eq} is a continuous control equal with the actual mean value of \mathbf{v} that can be estimated from \mathbf{v} using a low pass filter [4-6] - if possible without phase-delay. \mathbf{v}_{eq} from (8) contains valuable information on the required disturbance \mathbf{z} , but it depends on the system parameter uncertainties !

Remark. On the other hand, a disturbance compensation for the system (1) as $\mathbf{u} := \mathbf{u} - \mathbf{v}_{\text{eq}}$ using the equivalent control \mathbf{v}_{eq} (8) leads to an equivalent compensated system (9) without uncertain parameters and disturbance.

$$\begin{bmatrix} \dot{\mathbf{x}}_1 \\ \dot{\mathbf{x}}_2 \end{bmatrix} = \begin{bmatrix} \mathbf{A}_{11} & \mathbf{A}_{12} \\ \mathbf{A}_{21} & \mathbf{A}_{22} \end{bmatrix} \begin{bmatrix} \mathbf{x}_1 \\ \mathbf{x}_2 \end{bmatrix} + \begin{bmatrix} 0 \\ \mathbf{B}_2 \end{bmatrix} \mathbf{u}, \quad \begin{bmatrix} \mathbf{x}_1 \\ \mathbf{x}_2 \end{bmatrix}_{t=0} = \begin{bmatrix} \mathbf{x}_{10} \\ \mathbf{x}_{20} \end{bmatrix} \quad (9)$$

In conclusion, the sliding mode based observer for disturbance estimation (Fig.1) of the nonlinear system (1) is defined by the equation (2), with the discontinuous correction \mathbf{v} (3) that leads to sliding modes on switching surface $\boldsymbol{\sigma}$ (4). It has: inputs \mathbf{u} , eventual \mathbf{x}_1 ; estimated state

$$\tau < 1/(4 \dots 10 \omega). \quad (19)$$

$$\tau = 1/(4\omega), \text{ thus } K = 0.97, \Phi = -0.25 \text{ rad}. \quad (20)$$

ALPF1 digital implementation uses the bilinear (Tustin) method that leads to the discrete time equation (21), where $\mathbf{u} = \mathbf{v}$ and $\mathbf{y} = \mathbf{v}_{\text{eq}}$.

$$\mathbf{y}_k = \frac{1}{2+x} [2\mathbf{y}_{k-1} + x(\mathbf{u}_k + \mathbf{u}_{k-1} - \mathbf{y}_{k-1})], \quad (21)$$

$$x = 4h|\hat{\omega}|.$$

Other ALPF option uses a second order ALPF2 by serial connection of two ALPF1.

3.4. Phase-locked loop with sliding-mode state-observer

The equivalent control \mathbf{v}_{eq} from (15) contains sinusoidal components with desirable information on the speed and position. The first solution [5] to simply estimate the ω speed and θ position uses these components.

$$|\hat{\omega}_{\text{eq}}| = \sqrt{v_{\text{eq}\alpha}^2 + v_{\text{eq}\beta}^2} / \lambda_{\text{PM}}. \quad (22)$$

$$\hat{\theta} = -\tan^{-1}(v_{\text{eq}\alpha}/v_{\text{eq}\beta}). \quad (23)$$

The main disadvantages are the following:

- ω_{eq} speed estimation depends on the PMSM parameter uncertainties, especially λ_{PM} ,
- speed sign is not including, and this is a serious problem at zero speed crossing.

The second solution to estimate ω and θ uses a phase-locked loop (PLL) observer (Fig.3) [10]. The position error $\Delta\theta = \theta - \hat{\theta}$, is obtained from real part of the product $\mathbf{v}_{\text{eq}} e^{-j\hat{\theta}}$ expressed by:

$$v_{\text{eq}\alpha} \cos \hat{\theta} + v_{\text{eq}\beta} \sin \hat{\theta} = \omega \lambda_{\text{PM}} \sin \Delta\theta \cong \omega \lambda_{\text{PM}} \Delta\theta \quad (24)$$

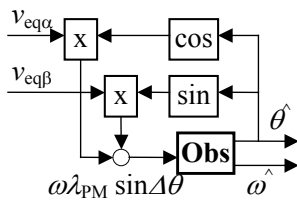


Fig.3. PLL observer structure.

For small $\Delta\theta$, $\sin \Delta\theta \approx \Delta\theta$, and the PLL system can be approached as a nonlinear control system [11] with variable gain $\omega \lambda_{\text{PM}}$.

The target of this tracking system is to drive the $\Delta\theta$ position error to zero with a very fast action. For these reasons, to estimate ω and θ , a

variable-structure PI state-observer (25) with relay switching function is used (Fig.4).

$$\begin{bmatrix} \hat{\theta} \\ \hat{\omega} \end{bmatrix}^* = \begin{bmatrix} 0 & 1 \\ 0 & 0 \end{bmatrix} \begin{bmatrix} \hat{\theta} \\ \hat{\omega} \end{bmatrix} + \begin{bmatrix} k_p \\ k_i \end{bmatrix} \text{sign } \Delta\theta, \quad \begin{bmatrix} \hat{\theta} \\ \hat{\omega} \end{bmatrix}_{t=0} = \begin{bmatrix} \hat{\theta}_0 \\ \hat{\omega}_0 \end{bmatrix}. \quad (25)$$

Because the ALPF1 give a constant phase-lag $\Phi = 0.25$ rad (20) for \mathbf{v}_{eq} , the position estimation θ_c^{\wedge} is simply compensate as $\theta_c^{\wedge} = \hat{\theta} + \Phi$.

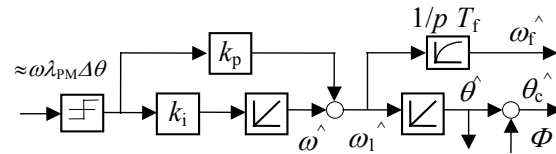


Fig.4. Variable-structure PI state-observer.

There are two possibilities for speed estimation: $\hat{\omega}$ and $\hat{\omega}_1$ [10], [12]. The $\hat{\omega}$ estimation is noiseless as output from the integrator. On the other hand, $\hat{\omega}_1$ estimation with the correction k_p has more accurate dynamic-estimation, but contains high frequency switching noises via k_p gain. To suppress noises, a LPF1 is added to obtain $\hat{\omega}_f$ estimation for the speed controller.

The voltage source inverter (VSI) consists on a three-phase bridge modeled by switching binary functions $S_a, S_b, S_c \in \{0,1\}$ delivered by the control system. In $\alpha\beta$ stator reference, the stator voltage vector \mathbf{u} has eight discrete values: $\mathbf{u} = 2/3 V_{\text{dc}} e^{jk\pi/3}$, $k = 0 \dots 5$, plus two null voltage vectors, where V_{dc} is the inverter dc-link voltage. Therefore, \mathbf{u} is computed as [10]:

$$\mathbf{u} = V_{\text{dc}} (2S_a - S_b - S_c)/3 + j V_{\text{dc}} (S_b - S_c)/\sqrt{3} \quad (26)$$

The sliding mode based observer complete structure for speed and position estimation is shown in Fig.5 with the following modules:

- EM+VSS – sliding-mode disturbance observer (Fig.2) and (13), (14),
- ALPF – adaptive low-pass filter (21),
- PLL observer (Fig.3) with variable-structure PI state-observer (Fig.4),
- 3/2 block – abc to $\alpha\beta$ reference operator,
- S/u – stator voltage vector computation (26).

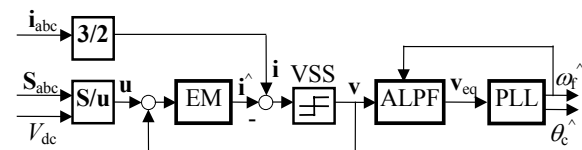


Fig.5. Sliding mode based observer structure.

4. SENSORLESS CONTROL

The sensorless control of PMSM drive structure (Fig.6) uses the proposed sliding mode based observer and contains the following modules:

- SM-Obs – sliding mode based observer,
- $R\omega$ – speed controller PI anti-windup type,
- dq to abc reference operator used in current vector control method with $i_d^* = 0$,
- Ri – phase-current controller bi-position type,
- VSI – voltage source inverter.

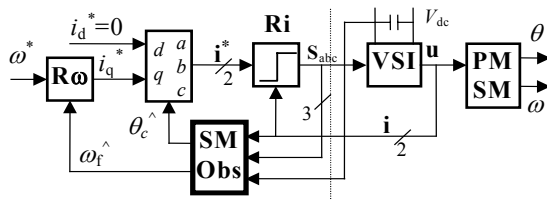


Fig.6. Sensorless control of PMSM drive system.

5. SIMULATION RESULTS

The parameters of the sensorless control for PMSM drive are the following:

- PMSM *rated data*: electromagnetic torque $T_e = 2.4$ Nm, stator current $I_a = 3$ A, mechanical speed $\omega = 1200$ rpm; and *rated parameters*: number of pole pairs $p = 4$, inertia $J = 0.005$ kgm², damping factor $B = 0.001$ Nms/rad, PM-flux $\lambda_{PM} = 0.1$ Wb, inductance $L = 0.02$ H, phase resistance $R = 1.8$ Ohm.
- VSI: dc-link voltage $V_{dc} = 100$ V, switching frequency $f_{inv} = 10$ kHz.
- Speed controller PI anti-windup with PT1 on speed reference ω^* : $T_{fo}^* = 60$ ms, $k_{p\omega} = 0.8$, $T_{i\omega} = 80$ ms, $k_{a\omega} = 10$, tuned after [13].
- Sliding mode based observer with PLL: $U_0 = 50$, $L_o=L$, $R_o=R$, $k_p = 50$, $k_i = 10^4$, $T_f = 10$ ms.

The dynamic performances of this sensorless drive are extensively investigated by digital simulation. The Matlab-Simulink package with Runge-Kutta 5th is used. The sampling rate $h = 50$ - 100 μ s, typically for IGBT inverters. The goal is to show robustness – especially $\Delta\theta$ convergence, for high and low speed, with load torque and real parameter variations.

For 80°C temperature variation, λ_{PM} decreases with 15%, and R increases with 30% [10]. The saturation phenomena decrease L , but the dependence $L(i)$ can be experimental determined

and implemented in the control system [1]. Thus, PMSM *detuned parameter case* are: $\lambda_{PM} = 0.85\lambda_{PM0}$, $R = 1.3R_o$, $L = 0.9L_o$.

The scenario for high and low speed is 1) $t_0 = 0$ s, step speed $\omega^* = \{1000, 30\}$ rpm; 2) $t_1 = 0.6$ s, step load torque $T_L^* = \{2.4, 0.6\}$ Nm, $h = \{100, 50\}$ μ s. In the tuned case, transient responses for ω , ω_f , $\theta - \theta_c$, T_e and i_a are shown in Fig.7 – for high speed, and in Fig.9 – for low speed. In detuned parameter cases, transient responses for ω and $\Delta\theta = \theta - \theta_c$ are shown in Fig.8 - for high speed, and in Fig.10 - for low speed.

Speed responses are fast, without steady state errors. The $\Delta\theta$ errors converge to zero in every case, proving the system robustness. The $\Delta\theta$ initial value is -15 deg, i.e., the ALPF1 compensation phase-lag Φ , and $\Delta\theta$ has a short period to reach convergence. The ω overshoot at low speed may be explained by the delay in ω estimation, and the stabilization from initial conditions in starting period. The ripple at low speed is maximum 5 rpm in permanent regime, but will decrease if the sampling rate is shorter.

The robustness to uncertainties in rotor inertia ($J = 3J_o$), for ω and $\Delta\theta$ transient responses are shown in Fig.11 – for high speed and Fig.12 – for low speed.

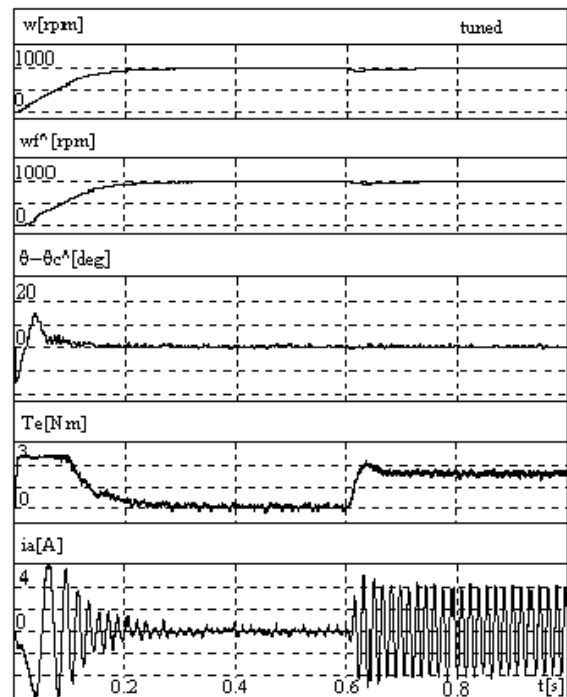


Fig.7. Transient responses ω , ω_f , $\theta - \theta_c$, T_e and i_a for steps $\omega^* = 1000$ rpm, $T_L^* = 2.4$ Nm, – tuned case.

In conclusion, the extensive simulation results prove the robustness of the proposed sliding

mode based observer in sensorless control of PMSM drive system, to real parameter variations, in 30-1000 rpm speed range.

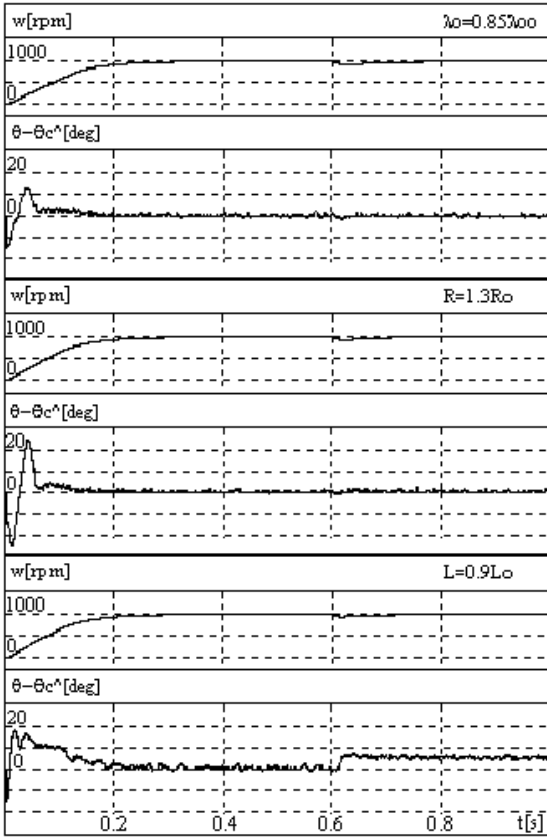


Fig.8. Transient responses ω , $\Delta\theta$ for steps $\omega^* = 1000$ rpm, $T_L^* = 2.4$ Nm, – detuned cases: a) $\lambda_{PM} = 0.85\lambda_{PM0}$, b) $R = 1.3R_0$, c) $L = 0.9L_0$.

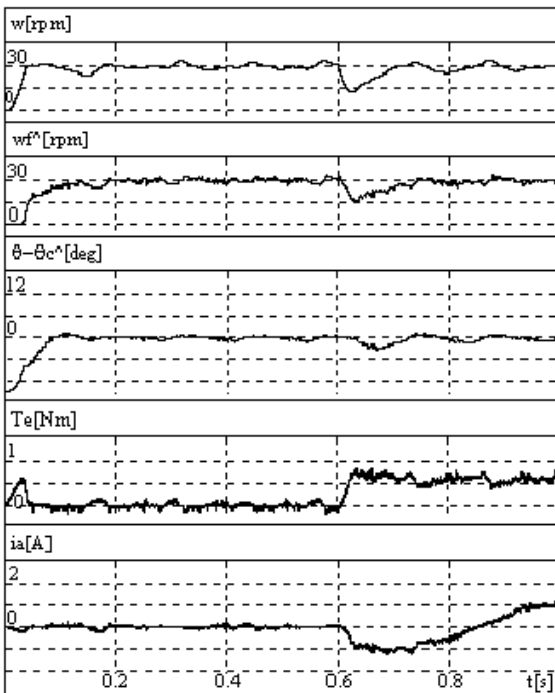


Fig.9. Transient responses ω , $\hat{\omega}$, $\theta - \hat{\theta}_c$, T_c and i_a for steps $\omega^* = 30$ rpm, $T_L^* = 0.6$ Nm, – tuned case.

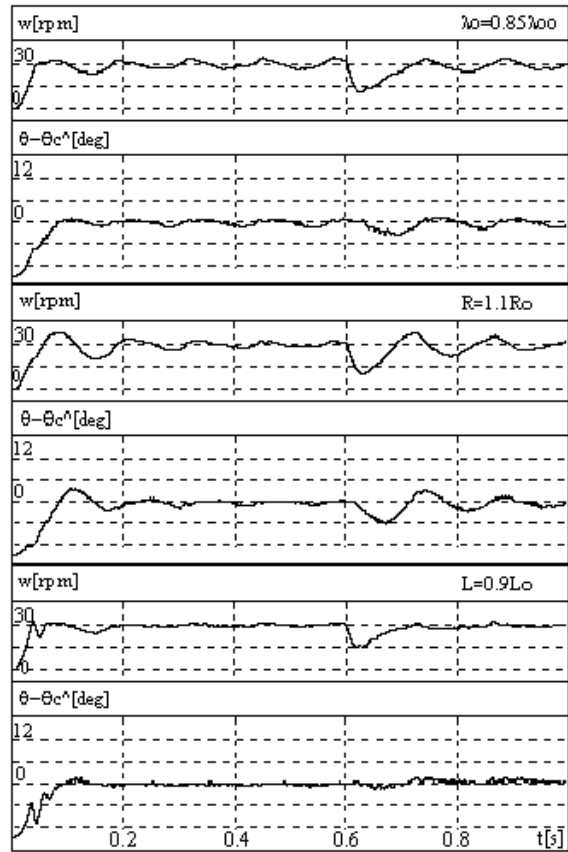


Fig.10. Transient responses ω , $\Delta\theta$ for steps $\omega^* = 30$ rpm, $T_L^* = 0.6$ Nm, – detuned cases: a) $\lambda_{PM} = 0.85\lambda_{PM0}$, b) $R = 1.1R_0$, c) $L = 0.9L_0$.

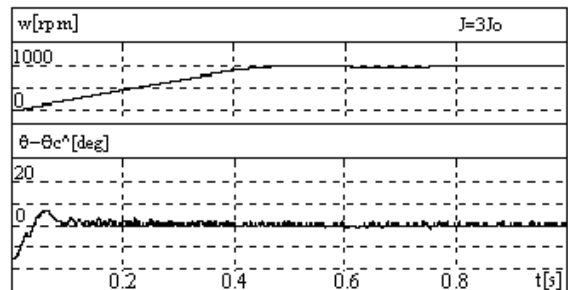


Fig.11. Transient responses ω , $\Delta\theta$ for steps $\omega^* = 1000$ rpm, $T_L^* = 2.4$ Nm, – detuned $J = 3J_0$.

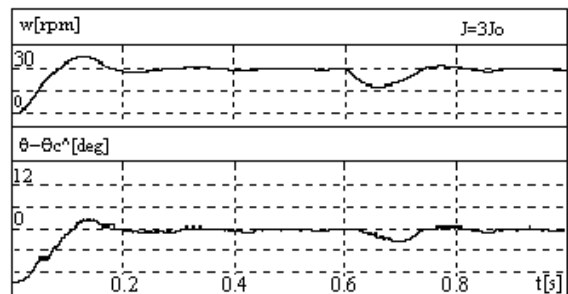


Fig.12. Transient responses ω , $\Delta\theta$ for steps $\omega^* = 30$ rpm, $T_L^* = 0.6$ Nm, – detuned $J = 3J_0$.

6. EXPERIMENTAL RESULTS

6.1. Hardware and software configuration

Hardware set-up of the experimental control system for PMSM drive (Fig.13) consists on: PC Pentium-166 MHz, ADA-1100 acquisition board 24 μsec / 12 bits ADC channel, adapter interface, power inverter. Required acquisition signals are: phase currents i_a, i_b and inverter dc-link voltage V_{dc} . The signals $\sin\theta, \cos\theta$ from a resolver position transducer (PT) are used to estimate θ and ω with a PLL observer only for monitoring. Output logic signals are S_a, S_b, S_c .

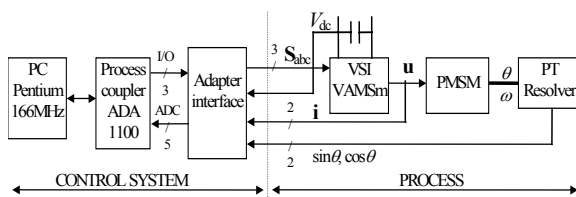


Fig.13. Experimental set-up for sensorless control.

Real time programs are divided in three parts:

- i) ADA-1100 resource administration (assembl),
- ii) Digital control and observer algorithms (C),
- iii) Off-line graphical display interface (C).

The real time system implements the sensorless control structure from Fig.6 with the sampling rate of $h = 200 \mu\text{s}$. A ring-buffer-list memorizes three desired variables used at the end of real time running by graphical display interface.

6.2. Experimental test results

The PMSM rated data and parameters are as in simulation results - chapter 5. The inverter switching frequency is 5 kHz, better than 2 kHz from the original analogue VAMS-m inverter.

The PMSM real parameters where determined by experimental methods [10]. A future possibility will be to tune the control system with the PMSM electromagnetic parameters by motor identification running during self-commissioning [2]. An automatic on-line tuning of inertia will be provided [3].

The *start-up procedure* uses a specific gate pattern to set the initial rotor position. The stator vector voltage sequence $S_{abc} = (100)$ and (000) is repeated five times with active/ pause time = 3/100 in ms. Therefore, the rotor automatically moves always to $\theta(0) = 0$.

The extensive digital simulation results (chapter 5) prepare the first set of parameters to tune the digital control algorithms implemented in experimental set-up. After that, they are fine tuned in practical experiments by trial and error procedure. The final parameter values are:

- Speed controller PI anti-windup with PT1 on ω^* : $T_{i\omega^*} = 60 \text{ ms}$, $k_{p\omega} = 0.1$, $T_{i\omega} = 90 \text{ ms}$, $k_{a\omega} = 10$.
- SMO with PLL: $U_0 = 50$, $L_o = L$, $R_o = R$, $k_p = 20$, $k_i = 2000$, $T_f = 10 \text{ ms}$, $\Phi = -0.25$.

Representative experimental tests are performed to explore the performances and limitations of the sensorless control for PMSM drive using the proposed sliding mode based observer.

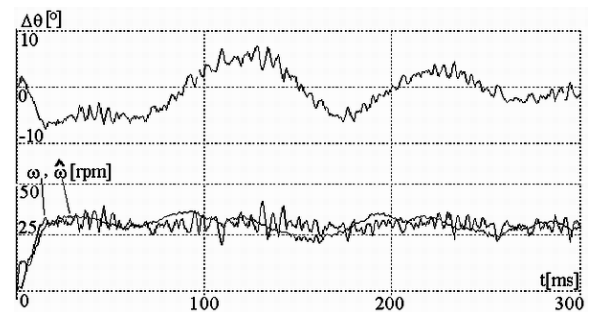


Fig.14. Transient responses $\Delta\theta, \omega, \hat{\omega}$ for step $\omega^* = 30 \text{ rpm}$, no loaded – experimental.

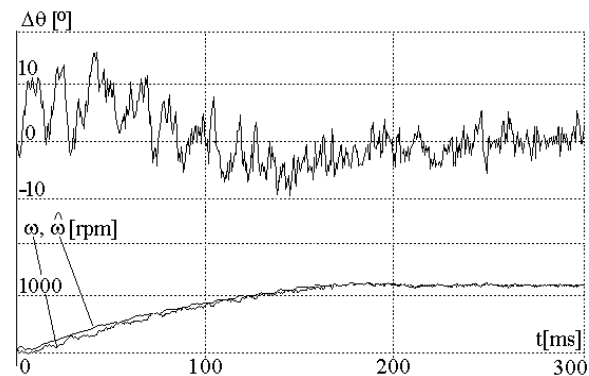


Fig.15. Transient responses $\Delta\theta, \omega, \hat{\omega}$ for step $\omega^* = 1200 \text{ rpm}$, no loaded – experimental.

The transient regimes are investigated at low speed $\omega^* = 30 \text{ rpm}$ (Fig.14), and high speed $\omega^* = 1200 \text{ rpm}$ (Fig.15) no loaded. For step speed start-up, there are presented transient responses of the position error $\Delta\theta$ and the mechanical speed: ω real speed, $\hat{\omega}$ estimated speed. The maximum position error $\Delta\theta = \pm 10 \text{ deg}$ and it rapidly converges to 0 deg.

7. CONCLUSIONS

The proposed observer structure to estimate the speed and position in sensorless PMSM drives contains two parts.

- i) A sliding-mode disturbance observer based on PMSM electrical model in stator reference, followed by an adaptive low-pass filter, estimates the equivalent control, i.e., the electromotive force vector (emf).
- ii) A phase-locked loop variable-structure PI observer extracts speed and position from emf.

A good idea is to use the equivalent disturbance given by the equivalent control in a disturbance controller not only for sensorless control.

The proposed observer demonstrates good performances in sensorless control of PMSM drive with current vector control method. The simulation results for real parameter variations prove the robustness of speed and position estimation. They show the observer asymptotic stability and good dynamic performances at high and low step speed, with step load torque. The experimental test results prove the feasibility of the proposed solution in 1:40 speed range.

This observer represents a promising solution that could be implemented in a DSP controller in order to be used in sensorless control of PMSM drives for medium speed range in industrial applications.

8. REFERENCES

- [1] Rajashekara, K., Kawamura, A. and Matsuse, K., (Eds.), - "Sensorless control of ac motor drives", IEEE Press, NJ, 1996.
- [2] Vas, P., - "Sensorless vector and direct torque control", Oxford University Press, Oxford, 1998.
- [3] Ohnishi, K., Matsui, N. and Hori, Y., - "Estimation, identification, and sensorless control in motion control systems", *Proc. of IEEE*, 82, **1253-1265**, 1994.
- [4] Utkin, V.I., Guldner, J. and Shi, J., - "Sliding mode control in electromechanical systems", Taylor & Francis, NY, 1999.
- [5] Ryvkin, S., - "Sliding-mode based observer for sensorless permanent magnet synchronous motor drive", *Proc. 7th Int. Power Electronics and Motion Control Conf. PEMC'96*, Budapest, 2, **558-562**, 1996.
- [6] Korondi, P., Young, D. and Hashimoto, H., - "Sliding mode based disturbance observer for motion control", *Proc. 37th IEEE Conf. on Decision and Control*, Tampa, FL, 2, **1926-1927**, 1998.
- [7] Chen, Z., Tomita, M., Doki, S. and Okuma, S., - "New adaptive sliding observer for position-and velocity-sensorless controls of brushless dc motors", *IEEE Trans. on Industrial Electronics*, 47, **582-591**, 2000.
- [8] Andreescu, G.D., Popa, A. and Spilca, A., - "Two sliding mode based observers for sensorless control of PMSM drives", *Electric Power Components and Systems Journal*, EPCS, Taylor & Francis Ltd., 30, **121-133**, 2002.
- [9] Buhler, H., - "Reglage par mode de glissement", Presses Polytechniques Romandes, Lausanne, 1986.
- [10] Andreescu, G.D., - "Estimators in control of electrical drives. Applications to permanent magnet synchronous motors" (in Romanian), Orizonturi Universitare Publisher, Timisoara, 1999.
- [11] Kaura, V. and Blasko, V., - "Operation of a phase locked loop system under distorted utility conditions", *IEEE Trans. on Industry Applications*, 33, **58-63**, 1997.
- [12] Lorenz, R.D., - "Observers and state filters in drives and power electronics", *Proc. 8th Int. Conf. on Optimization of Electrical and Electronic Equipment OPTIM 2002*, Brasov, Keynote, **XIX-XXVIII**, 2002.
- [13] Preitl, S. and Precup, R.-E., - "An extension of tuning relations after symmetrical optimum method for PI and PID controllers", *Automatica*, 35, **1731-1736**, 1999.